

Photoconductivity of evaporated amorphous silicon films post-hydrogenated in a theta-pinch plasma

K. P. Chik and P. K. Lim

Department of Physics, The Chinese University of Hong Kong, New Territory, Hong Kong

B. Y. Tong, P. K. John, and P. K. Gogna

*Department of Physics and Centre for Interdisciplinary Studies in Chemical Physics,
The University of Western Ontario, London, Ontario N6A 3K7, Canada*

S. K. Wong

Department of Chemistry, The University of Western Ontario, London, Ontario N6A 5B7, Canada

(Received 17 May 1982; revised manuscript received 19 October 1982)

Evaporated amorphous silicon films treated in a theta-pinch hydrogen plasma (hereafter TPH films) show good photoconductivity. The Staebler-Wronski instability is absent in such films. The dark conductivity and photoconductivity are measured. The dependence of photoconductivity on temperature and on intensity of light illumination has been investigated. From the analysis it is found that from 373 K down to liquid-nitrogen temperature mainly two kinds of recombination mechanisms are responsible for photoconductivity in TPH films. The recombination kinetics associated with an activation energy of 0.28 ± 0.01 eV is of second order and that with an activation energy of 0.08 ± 0.01 eV is of first order. The wavelength dependence of the photocurrent gives an estimated optical gap of 1.6–1.7 eV for TPH films.

I. INTRODUCTION

Photoconductivity measurements provide a simple way of obtaining information about transport mechanism in a semiconductor. Such measurements have been applied successfully by Spear and co-workers¹ to study amorphous silicon (*a*-Si) films produced by the glow discharge of silane. These films exhibit good photoresponse. By analyzing the temperature dependence of steady-state photoconductivity in their films, Spear and co-workers established a basic model for *a*-Si. According to their interpretation, the photocurrent above 250 K is carried by electrons in the extended states with an activation energy of 0.18 eV, while transport below this temperature is by phonon-assisted hopping through states near the bottom of band-tail states with a much smaller activation energy of 0.08 eV.

It is known that properties of glow-discharge *a*-Si films depend sensitively on the plasma condition during film formation and it is difficult to control all the parameters in the complex reaction taking place during silane decomposition.² Published results from different laboratories show significant differences in the details of photoconductivity.^{3–5} The situation is further complicated by the presence of the Staebler-Wronski effect⁶ which was unknown in earlier investigations. Furthermore, there is the

problem of hydrogen evolution on heating the glow-discharge *a*-Si films, indicating that some hydrogen atoms are probably loosely bound in the amorphous matrix.⁷ The Staebler-Wronski instability is seen as a major difficulty in the application of *a*-Si in semiconductor devices.⁸

In spite of the difficulties mentioned above, the glow-discharge *a*-Si films are still the most actively pursued. On the other hand, *a*-Si films obtained by vacuum evaporation, while showing very little or no photoresponse, can be made photoconducting by modification by hydrogenation since hydrogen can sweep clean the energy gap.^{9–11} For example, Ghosh *et al.*¹² tried to coevaporate silicon with hydrogen, but the film properties were not satisfactory. Early attempts to posthydrogenate evaporated *a*-Si films have met with little success. LeComber *et al.*¹³ found that even after 9 h of treatment in a hydrogen discharge both the conductivity and activation energy remained the same. However, the electron-spin-resonance signal had been reduced to a level below their detection limit of $5 \times 10^{17} \text{ cm}^{-3}$.¹⁴ The first effective posthydrogenation was reported by Kaplan *et al.*¹⁵ in which films freshly deposited in ultrahigh vacuum were hydrogenated in a hydrogen glow discharge. Tong *et al.*¹⁶ recently demonstrated that *a*-Si films evaporated in an ordinary vacuum of $\sim 10^{-7}$ Torr can be successfully post-

hydrogenated by treating the evaporated films in a theta-pinch hydrogen plasma (hereafter TPH films). TPH films show good optical and electrical properties, comparable to those of the glow-discharge films, and in addition they are highly stable exhibiting no Staebler-Wronski effect. This paper is a first attempt to present detailed studies of the dependence of the steady-state photoconductivity on temperature and light intensity in TPH films. The TPH films are posthydrogenated films, and thus are different from films produced by incorporating hydrogen into the *a*-Si during film formation.

II. EXPERIMENTAL METHODS

Films of *a*-Si typically 6000 Å thick were prepared by evaporation from Si powder (supplied by Balzers) using an electron gun in a conventional high-vacuum coating unit. Coating rate was 2 Å/s and the substrate was Corning 7059 glass. After evaporation the *a*-Si films were hydrogenated in a theta-pinch plasma machine as described in an earlier report.¹⁷ The photoconductivity σ_p , which is defined as the difference between conductivity under illumination σ_L and the dark conductivity σ_D , was measured between two silver or aluminum electrodes 2 mm apart under an electric field of about 100 V/cm using a Keithley 640 electrometer. For optical excitation a tungsten-halogen lamp or He-Ne laser with appropriate filters were used. A xenon arc lamp in conjunction with a Spex single-beam monochromator was used as the usual light source when studying spectral dependence of the photocurrent. The temperature of the sample was controlled by a stream of warm or cold nitrogen gas, so that the temperature dependence of σ between 420 and 140 K was measured at a cooling rate of less than 1 K/min.

The stability of TPH films made it possible to take accurate readings with slow cooling rate and long waiting time for the sample to reach thermal equilibrium with the surroundings. The same sample was used in the many cycles of heating and cooling as required in the temperature- and intensity-dependence measurements. The same samples were used in other measurements such as optical-absorption and lifetime studies. Results of the latter require further analysis and will be presented later.

III. EXPERIMENTAL RESULTS

A. Dark conductivity

The temperature dependence of σ_D of the evaporated films before hydrogenation shows similar behavior as reported earlier.^{18,19} Conduction is predominantly by hopping in the temperature range

between 140 and 343 K. Above 343 K extended conduction becomes important with an activation energy between 0.7 and 0.8 eV.

After hydrogenation for the TPH films, the plot of $\ln\sigma_D$ against $1/T$ can be fitted to two straight lines of different slopes. A typical plot is the dashed curve shown in Fig. 1. The entire temperature dependence of σ_D can be described by the sum of two exponential functions, namely

$$\sigma_D = \sigma_{1D} \exp(-E_{1D}/kT) + \sigma_{2D} \exp(-E_{2D}/kT). \quad (1)$$

The first term has been interpreted to describe a conduction mechanism in the extended states of the conduction band, whereas the second term has been attributed to nearest-neighbor hopping conduction.¹⁸ From Fig. 1 one sees immediately that in TPH films the transition from the first to the second mechanism occurs at a temperature of about 260 K and this is much lower than that for unhydrogenated films. The parameters for several TPH *a*-Si films are listed in Table I. We see from the table that all the TPH films have very similar prop-

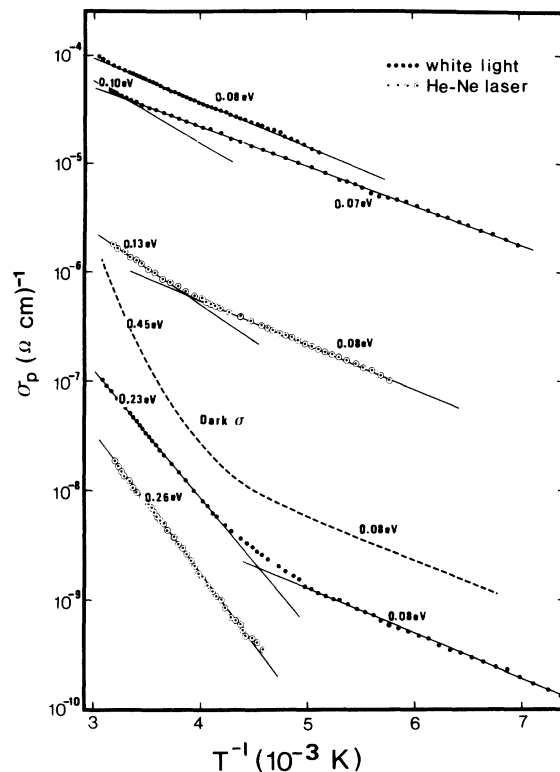


FIG. 1. Temperature dependence of photoconductivity σ_p at different intensities of light illumination. At the same temperature σ_p is larger for the higher intensity. Dashed curve is the dark conductivity σ_D (sample *b*).

TABLE I. Parameters obtained from dark-conductivity measurements of TPH films.

Sample	E_{1D} (eV)	σ_{1D} ($\Omega^{-1}\text{cm}^{-1}$)	E_{2D} (eV)	σ_{2D} ($\Omega^{-1}\text{cm}^{-1}$)	σ (20°C) ($\Omega^{-1}\text{cm}^{-1}$)
<i>a</i>	0.44	13	0.10	4×10^{-7}	3.8×10^{-7}
<i>b</i>	0.45	10	0.08	6×10^{-7}	2.1×10^{-7}
<i>c</i>	0.42	2	0.13	2×10^{-6}	1.2×10^{-7}
<i>d</i>	0.49	44	0.15	6×10^{-6}	1.9×10^{-7}
<i>e</i>	0.53	27	0.14	1×10^{-6}	2.5×10^{-8}

erties. E_{1D} which was measured to be ~ 0.75 eV before hydrogenation drops to about 0.45 eV for the TPH films, whereas E_{2D} is only slightly affected by hydrogenation. Since E_{1D} represents the activation energy for extended conduction, hydrogenation is thus effectively seen to shift the Fermi level towards the band edge. E_{2D} represents the activation energy associated with hopping conduction and therefore is less affected. Thus the room-temperature σ_D of TPH films is higher than that of the unhydrogenated films and is 2 orders of magnitude higher than that of silane glow-discharge films.

B. Absence of the Staebler-Wronski effect

The TPH films are highly photosensitive. Under white-light illumination of intensity 200 mW/cm^2 , σ_P reaches a value $\sim 10^{-4} \Omega^{-1}\text{cm}^{-1}$ with no sign of saturation yet. This value is comparable with that for glow-discharge films. On the other hand, it has already been demonstrated that TPH films show no change in σ_P after light illumination for long periods of time.¹⁶ In order to examine whether the TPH films are in a metastable state after strong light exposure for a long time as described by Staebler and Wronski,⁴ several samples were heated to 423 K for 4 h and others to 673 K for 2 h. No changes in dark or photoconductivity have been observed as a result. Observations were repeated for TPH films doped with phosphorous with an activation energy of 0.2 eV and again no changes were detected. The Staebler-Wronski instability is thus absent in the TPH films.

C. Dependence of σ_P on temperature

Figure 1 shows the temperature dependence of σ_P for different intensities of light illumination for sample *b*. The curve at the top corresponds to an incident white-light intensity of 200 mW/cm^2 . The middle and bottom curves correspond to incident intensities of 2 mW/cm^2 and $3 \mu\text{W/cm}^2$ of He-Ne light, respectively. The results described below are highly reproducible from sample to sample. In this paper only data on samples *b* and *c* are quoted as

typical examples.

Except for the highest and lowest intensity of illumination used (i.e., the top and bottom curves) all the $\ln\sigma_P$ -vs- $1/T$ plots can be well approximated by two straight lines of different slopes for the temperature range between 373 and 133 K. Assuming that a single conduction mechanism is present in a particular region, this region can be well represented by the equation

$$\sigma_P = \sigma_0 \exp(-\epsilon/kT). \quad (2)$$

The slope of $\ln\sigma_P$ -vs- $1/T$ plots gives the appropriate ϵ values which are labeled on the curves in Fig. 1. From the figure we see that in the low-temperature range, $\epsilon \approx 0.08$ eV for all light intensities investigated and it remains at this constant value for other samples as well, despite some fluctuation in E_{2D} of σ_D .

In the high-temperature range, ϵ is seen to depend strongly on the intensity of illumination. From Fig. 1, ϵ is seen to decrease steadily from 0.26 to 0.1 eV as intensity is increased by 5 orders of magnitude. The temperature of transition from one region to the other shifts to higher values as the light intensity is increased. Such intensity dependence of ϵ and shift in transition temperature have not been reported previously in glow-discharge samples. It is not easy to explain these observations satisfactorily if we insist on the assumption that each region is represented by a single mechanism as in Eq. (2). For this reason, we do not regard the values ϵ as "activation energies" (see Sec. IV).

D. Dependence of i_p on intensity

The dependence of photocurrent i_p on light intensity I at room temperature for five decades of intensity change is plotted in Fig. 2. The experimental point with the highest i_p value corresponds to a light illumination of 2-mW/cm^2 He-Ne laser light. It has the form

$$i_p \propto I^\gamma. \quad (3)$$

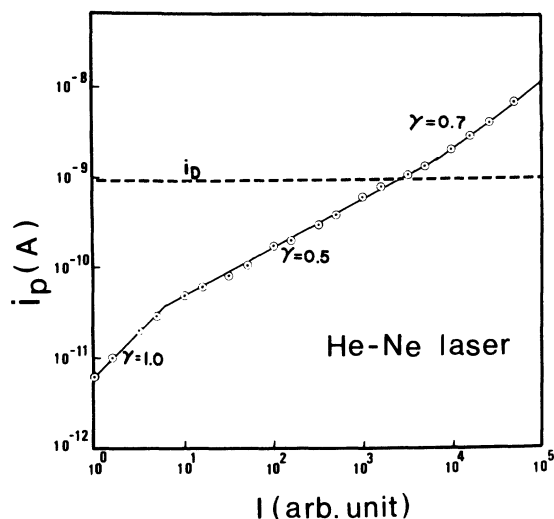


FIG. 2. Dependence of photocurrent i_p on light intensity at RT using a He-Ne laser as light source.

The curve in Fig. 2 separates into three distinct regions. At very low intensity, $\gamma=1$, indicating a first-order type of recombination. Spanning a wide range of medium intensity, γ is 0.5, indicating a second-order type of recombination. Finally at high intensity, γ becomes 0.7 which reflects a more complicated type of recombination process.

There is a further detail that has not been reported before. We observe that in the high intensity regime, the value of γ does not stay at 0.7 but increases slowly. Instead of raising the light intensity further which may introduce complications, the contribution from the second-order recombination process could be suppressed by lowering the temperature. The reason that we can do so will become clear from the analysis presented in the next section (Sec. IV). Figure 3 shows how $\log_{10} i_p$ changes with intensity I at room temperature (RT) and at 152 K as shown in the top and bottom curves, respectively. Upon lowering the temperature γ increases from 0.68 to 0.79.

In all the above experiments (Secs. III C and III D) there is no significant difference between using a monochromatic light source, for example, a He-Ne laser ($\lambda=6328 \text{ \AA}$), or white light. There is no field effect within the range 20–800 V applied across a gap of 2 mm. Normally, an electric field of about 100 V/cm was used.

E. Photocurrent dependence on wavelength

Following Loveland *et al.*²⁰ the optical gap could be estimated by plotting $(i_p h\nu/N_0)^{1/2}$ vs $h\nu$, where i_p is the photocurrent, $h\nu$ is the photon energy, and N_0 is the total number of incident photons per

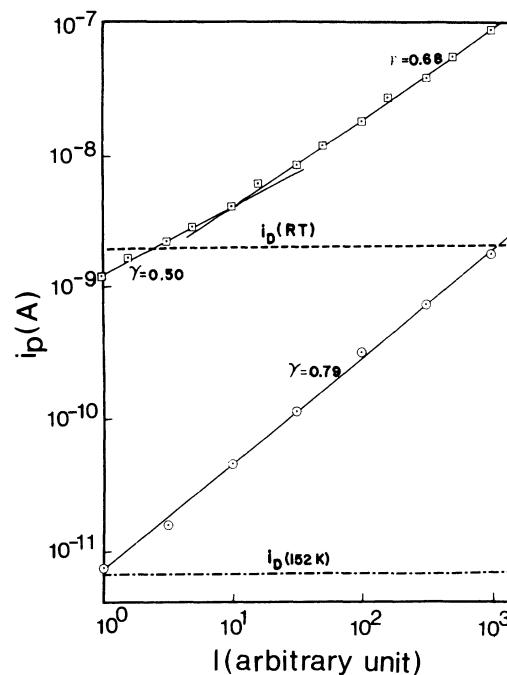


FIG. 3. Dependence of photocurrent i_p on light intensity at RT and at 152 K using a white light source. i_D is the dark current of sample *b* at the temperature indicated. Field across the electrodes is about 250 V/cm.

square centimeter per second under condition that $\gamma=1$. Figure 4 shows such a plot for the TPH films, where $\gamma=1$ was assured because of the low intensity of our light source used in this case. From the figure the optical gap is found to lie between 1.6 and 1.7 eV and this is the same as the result reported for glow-discharge samples.

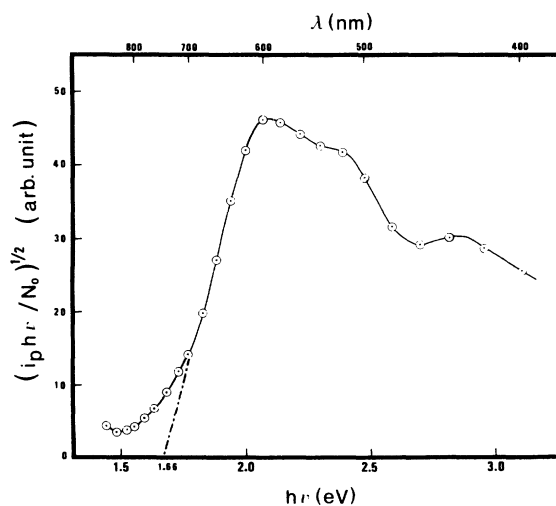


FIG. 4. Photocurrent i_p dependence on incident-photon energy $h\nu$. N_0 is the total number of incident photons/cm².

IV. ANALYSIS OF RESULTS

According to Fig. 1 dependence of σ_P on temperature can be divided in general into two regions, each region showing an exponential dependence on $1/T$. These results can be summarized in the following equation:

$$\sigma_P = \sigma_1 + \sigma_2 = \sigma_{01} \exp(-E_1/kT) + \sigma_{02} \exp(-E_2/kT). \quad (4)$$

If one can measure σ_P over a wide enough temperature range, the two regions can be completely separated and the slopes of the linear plots in Fig. 1 can give the right values of activation energy E . If, however, the temperature range covered is small, say, for example, in the high-temperature region, one may be measuring σ_P in a temperature range where both σ_1 and σ_2 contribute. This can happen even when the $\ln\sigma_P$ -vs- $1/T$ plot apparently shows a straight line. The activation energy obtained in such case can be considered as an effective activation energy only. The monotonic decrease in ϵ_1 in region I with increasing light intensity leads us to suspect that ϵ_1 [see Eq. (2)] may not be the true values of E_1 in Eq. (4). Hence we reanalyzed our results by decomposing σ_P into two components according to Eq. (4). It is obvious that if we can measure σ_P down to a low enough temperature, the contribution of σ_1 to σ_P will become insignificant and we can use this part of the curve to determine σ_2 . Figure 1 shows that this is really the case since all curves in region II have the same value $\sigma_2=0.08$ eV. Putting $\epsilon_2=E_2$ and using the measured values of σ_P , the values of E_1 , σ_{01} , and σ_{02} are varied until all experimental points fit into two straight lines in the $\ln\sigma$ -vs- $1/T$ plots. Figures 5 and 6 illustrate the results of such decomposition for two cases at different light intensities. Two different samples are selected so as to show that the analysis is sample independent. Figure 7 further illustrates such decomposition done on the same sample for four different photon fluxes, namely 9×10^{12} , 8×10^{13} , 8×10^{14} , and 2×10^{15} photons/cm²s from a He-Ne laser. One can see that such decomposition works excellently for all experimental curves measured. Most significantly the value of E_1 was found to be constant, independent of light intensity. Hence we can conclude that for TPH films, there exist two different recombination processes which are coexistent over a wide range of temperature. The activation energies for these two processes are, respectively, in units of eV,

$$E_1 = 0.28 \pm 0.01$$

and

$$E_2 = 0.08 \pm 0.02.$$

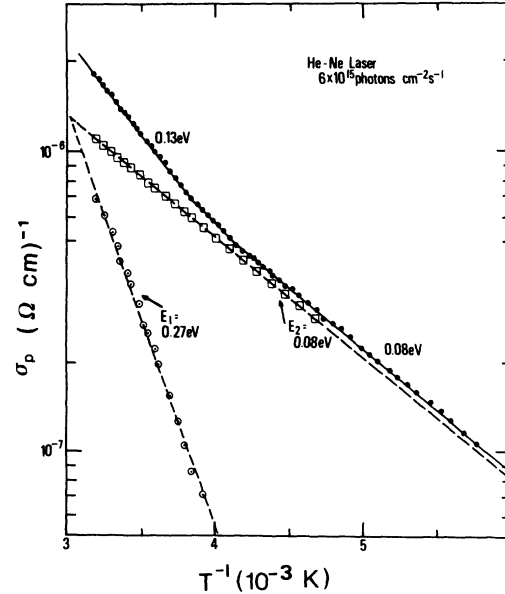


FIG. 5. Temperature dependence of σ_P for a photon flux of 6×10^{15} photons/cm²s from a He-Ne laser on sample *b*. In this case σ_P is larger than σ_D . Two straight lines are obtained by decomposing the measured curve into two exponentials as described in the text. E_1 and E_2 are activation energies [see Eq. (4)].

Since both E_1 and E_2 are intensity independent, the intensity dependence of σ_P must appear only in the coefficients σ_{01} and σ_{02} .

Let σ_{01} be proportional to intensity to the power γ'_1 ,

$$\sigma_{01} \propto I^{\gamma'_1}, \quad (5)$$

and similarly let σ_{02} be proportional to intensity to the power γ'_2 . We have

$$\sigma_{02} \propto I^{\gamma'_2}. \quad (6)$$

A plot of $\log_{10}\sigma_{01}$ and $\log_{10}\sigma_{02}$ versus intensity for the four curves shown in Fig. 7 gives $\gamma'_1=0.44$ and $\gamma'_2=0.93$ (Fig. 8). Similar plots for other samples also give γ'_1 close to 0.5 and γ'_2 close to 1.0. Considering the numerical uncertainty involved in curve fitting, these values indicate that the first term in Eq. (4) has second-order-type recombination kinetics and the second term has first-order type. In view of the above analysis, one can write empirically for the TPH films,

$$\sigma_P = a_1 I^{1/2} e \mu_1 \exp(-E_1/kT) + a_2 I e \mu_2 \exp(-E_2/kT), \quad (7)$$

where μ_1 and μ_2 are the corresponding mobilities.

The above analysis also enables us to explain the variation of σ_P in the high-intensity regime. The

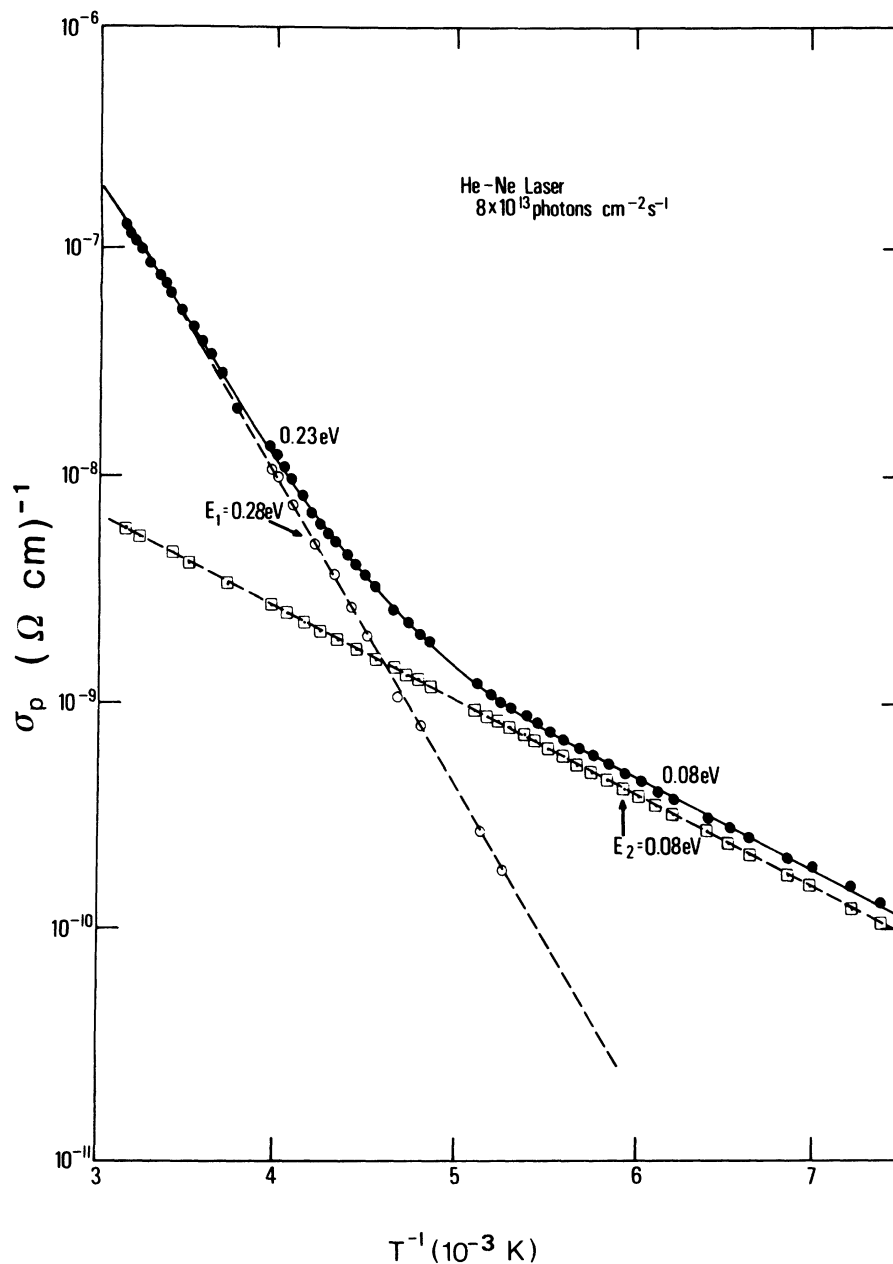


FIG. 6. Temperature dependence of σ_p for a photon flux of 8×10^{13} photons/cm²s from a He-Ne laser on sample *c*. In this case, σ_p is lower than σ_D . Two straight lines are obtained by decomposing the measured curve into two exponentials as described in the text. E_1 and E_2 are activation energies [see Eq. (4)].

case $\gamma=0.7$ in the high-intensity regime in Fig. 2 is due to the simultaneous contribution of the two terms. As intensity increases, the second term, being proportional to I , contributes more and more giving a slowly increasing effective γ in i_p defined in Eq. (3). The increasing contribution from the second term with increasing intensity naturally pushes the transition temperature towards the high-temperature

side (Fig. 1). The shift in transition temperature with increasing intensity is thus automatically explained. Furthermore, one sees that the true value for γ is only obtained in the temperature and intensity range where only one recombination process is predominant. Clearly, RT is not the right temperature for such measurements in the high-intensity range of Fig. 2.

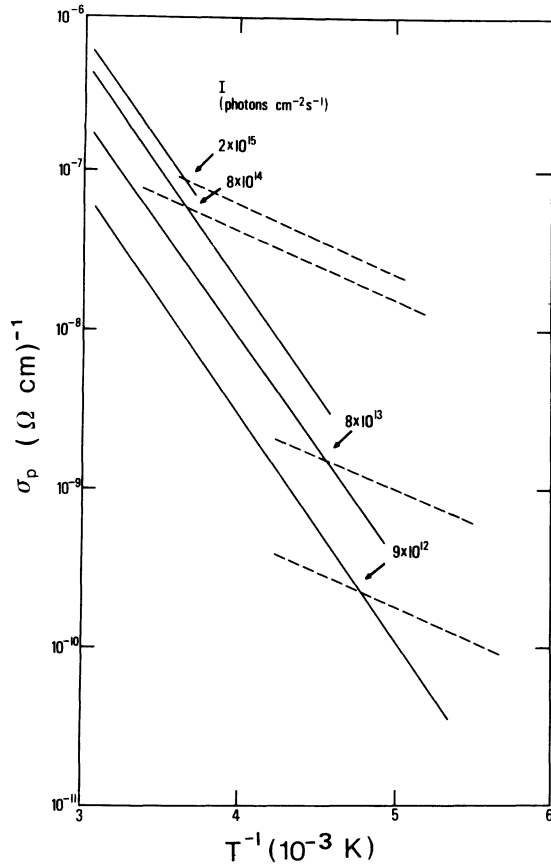


FIG. 7. σ_p -vs- $1/T$ curves decomposed into two components σ_1 and σ_2 [Eq. (4)] at four different photon fluxes: 2×10^{15} , 8×10^{14} , 8×10^{13} , and 9×10^{12} photons/cm²s. All curves show the same activation energies: $E_1 = 0.28$ eV and $E_2 = 0.08$ eV. The sample is c.

V. DISCUSSION

One would not expect that a conclusive recombination model can be derived solely from photoconductivity measurements. Therefore, we do not elaborate on a detailed recombination model. However, by comparing our results with other recombination models proposed for glow-discharge films,^{1,20-23} we can profitably gain insight into some possible physical processes. There are some features common between our results and those of the high-temperature deposition glow-discharge films.¹ For example, region I of the TPH films has the same intensity dependence for σ_p as region B in the glow-discharge films, while region II in our case has identical activation energy as that for region C in the glow-discharge films. According to the recombination model of Spear *et al.*,¹ a shallow electron-trapping level is situated at $\epsilon_A \approx 0.2$ eV below ϵ_C while another group of localized states involved in the recom-

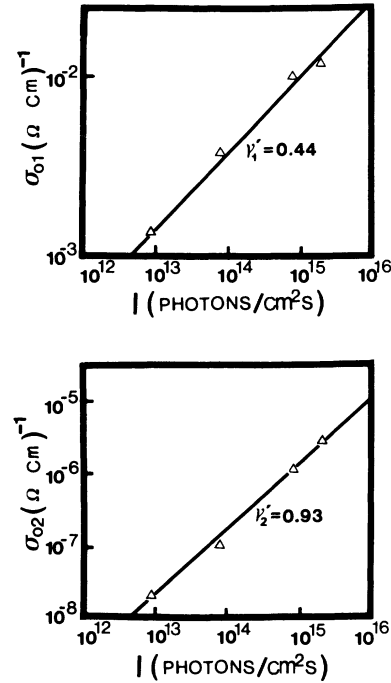


FIG. 8. The prefactors σ_{01} and σ_{02} of σ_1 and σ_2 [Eq. (4)] obtained from the decomposition of the four curves in Fig. 7 are plotted against I , the photon flux. From these plots, we see that $\gamma'_1 = 0.44$ and $\gamma'_2 = 0.93$, where γ'_1 and γ'_2 are defined in Eqs. (5) and (6), respectively.

ination process is assumed to be at $\epsilon_y \approx 1.1$ eV below ϵ_C . ϵ_C is the energy at which extended conduction becomes important. If the photogenerated density of carriers at ϵ_C is far larger than that in the dark, i.e., if $\sigma_p \gg \sigma_D$, one expects the neutrality condition to hold, with approximately an equal number of negatively charged centers at A and positively charged centers at y . Assuming the predominant recombination path to go between ϵ_A and ϵ_y , one obtains¹

$$\sigma_p \propto I^{1/2} \exp[-(\epsilon_C - \epsilon_A)/kT], \quad (8)$$

where I is the light intensity incident on the film. This equation predicts, for high light intensity, an activation energy of $\epsilon_C - \epsilon_A$ for $\gamma = 0.5$.

At low temperature, the electron hops to a neighboring atom with phonon assistance at ϵ_A . Equation (8) now becomes

$$\sigma_p \propto I^{1/2} \exp(-W/kT). \quad (9)$$

The temperature at which transition from recombination between photogenerated carriers and traps at ϵ_A to the hopping mechanism along ϵ_A occurs is found by equating Eqs. (8) and (9). Since both equations depend on $I^{1/2}$, the transition temperature

would appear to be clearly intensity independent. This recombination model clearly contradicts our results in two respects, namely, the intensity dependence of the transition temperature between regions I and II and the first-order recombination kinetics in region II. As is pointed out already in Sec. IV, the intensity dependence of the transition temperature is a direct consequence of two different recombination processes. Because Eq. (9) does not predict the correct intensity dependence for the TPH films, the hopping mechanism does not apply to this type of film. The first-order recombination kinetics observed in TPH films at low temperature is very similar to the behavior in chalcogenides.²⁴ The explanation of the latter is that carriers (usually holes) fall into traps and do not get out before recombination takes place. We may similarly assume that holes excited by light radiation are easily trapped by recombination centers and quickly recombine with carriers at the conduction band so that the trapped-hole concentration is approximately constant. In this way we would expect first-order recombination kinetics. Similar observation was reported by Hoheisel *et al.*²³

There is another case where a first-order recombination process is observed in TPH films (see Fig. 2). Here the photocurrent is 2 orders of magnitude smaller than the dark current when the light intensity is extremely low. This result can be explained in the usual way that thermal effect overpowers the photogeneration effect²⁴⁻²⁷ without the introduction of a third transition mechanism. This should not be confused with the first-order kinetics observed in the high-light-intensity regime at low temperature.

The interpretation of the results in the high-temperature regime in TPH films appears simpler. The intensity dependence of the photocurrent can be accounted for by Eq. (8). If one accepts this recom-

bination process, one can readily identify E_1 as

$$E_1 = \epsilon_C - \epsilon_A = 0.28, \quad (10)$$

in eV, which is larger than that observed in glow-discharge films.¹ This would indicate that the TPH films probably have a larger band tail than the glow-discharge films. One has to be careful about this interpretation since one can easily devise other recombination models which give also second-order recombination kinetics. Hence other experiments have to be designed to confirm the above interpretation.

VI. CONCLUSION

The TPH films are highly photosensitive and stable. Their properties can be easily reproduced. Analysis of photoconductivity results shows that the TPH films behave differently in some respects from the glow-discharge films. This is most apparent in the low-temperature, high-light-intensity regime. The photoconduction mechanism in this region (region II) cannot be reconciled with a phonon-assisted-hopping conduction around ϵ_A as proposed by Spear *et al.*¹ for the glow-discharge films. One would rather suggest that both types of excited carriers (electrons and holes) can take part in the recombination process so that two recombination mechanisms may coexist. Owing to the difference in the physical properties of the two carriers, one mechanism may predominate at high temperature while the other becomes important at low temperature where the high-temperature mechanism is strongly suppressed. The difference in properties between TPH films and glow-discharge films indicates that the gap structure of these two kinds of films may not be the same. This is not surprising in view of the complete difference in the film-preparation procedures.

¹W. E. Spear, R. J. Loveland, and A. Al-Sharbaty, *J. Non-Cryst. Solids* **15**, 410 (1974).

²W. E. Spear and P. G. Le Comber, in *Proceedings of the Seventh International Conference on Amorphous and Liquid Semiconductors, Edinburgh, 1977*, edited by W. E. Spear (University of Edinburgh Press, Edinburgh, 1977), p. 309.

³P. J. Zanzucchi, C. R. Wronski, and D. E. Carlson, *J. Appl. Phys.* **48**, 5227 (1977).

⁴D. E. Carlson and C. R. Wronski, in *Amorphous Semiconductors*, edited by M. H. Brodsky (Springer, New York, 1979), p. 287.

⁵W. Fuhs, M. Milleville, and J. Stuke, *Phys. Status Solidi B* **89**, 495 (1978).

⁶D. L. Staebler and C. R. Wronski, *Appl. Phys. Lett.* **31**,

292 (1977).

⁷H. Fritzsche, in *Proceedings of the Seventh International Conference on Amorphous and Liquid Semiconductors, Edinburgh, 1977*, Ref. 2, p. 3.

⁸D. Adler, *J. Non-Cryst. Solids* **42**, 315 (1980).

⁹F. C. Choo and B. Y. Tong, in *Proceedings of the Seventh International Conference on Amorphous and Liquid Semiconductors, Edinburgh, 1977*, Ref. 2, p. 120.

¹⁰F. C. Choo and B. Y. Tong, *Solid State Commun.* **25**, 385 (1978).

¹¹T. D. Moustakas, D. A. Anderson, and W. Paul, *Solid State Commun.* **23**, 155 (1977).

¹²A. K. Ghosh, T. McMahon, E. Rock, and H. Wiesmann, *J. Appl. Phys.* **50**, 3407 (1979).

¹³P. G. LeComber, A. Madan, and W. E. Spear, *J. Non-*

- Cryst. Solids **11**, 219 (1972).
- ¹⁴P. G. LeComber, R. J. Loveland, W. E. Spear, and R. A. Vaughan, in *Proceedings of the Fifth International Conference on Amorphous and Liquid Semiconductors, Garmisch-Partenkirchen, 1973* (Taylor and Francis, London, 1974), p. 245.
- ¹⁵D. Kaplan, N. Sol, G. Velasco, and P. A. Thomas, *Appl. Phys. Lett.* **35**, 440 (1978).
- ¹⁶B. Y. Tong, P. K. John, S. K. Wong, and K. P. Chik, *Appl. Phys. Lett.* **38**, 789 (1981).
- ¹⁷P. K. John, S. K. Wong, P. K. Gogna, B. Y. Tong, and K. P. Chik, in *Proceedings of the Ninth International Conference on Amorphous and Liquid Semiconductors, Grenoble, 1981* [*J. Phys. (Paris) Colloq.* **42**, Suppl. No. 10, C4-639 (1981)].
- ¹⁸K. P. Chik, S. Y. Feng, and S. K. Poon, *Solid State Commun.* **33**, 1019 (1980).
- ¹⁹S. K. Poon and M. Phil, thesis, The Chinese University of Hong Kong, 1978 (unpublished).
- ²⁰R. J. Loveland, W. E. Spear, and A. Al-Sharbaty, J. Non-Cryst. Solids **13**, 55 (1973/1974).
- ²¹W. E. Spear, H. Al-Ani, and P. G. LeComber, *Philos. Mag. B* **43**, 781 (1981).
- ²²W. E. Spear, D. Allan, P. LeComber, and A. Ghaith, *Philos. Mag. B* **41**, (1980).
- ²³B. Hoheisel, R. Fischer, and J. Stuke, in *Proceedings of the Ninth International Conference on Amorphous and Liquid Semiconductors, Grenoble, 1981* [*J. Phys. (Paris) Colloq.* **42**, Suppl. No. 10, C4-819 (1981)].
- ²⁴N. F. Mott and E. A. Davis, *Electronic Processes in Non-Crystalline Materials* (Clarendon, Oxford, 1979), p. 259.
- ²⁵P. Nagels, in *Amorphous Semiconductors*, Ref. 4, p. 113.
- ²⁶T. C. Arnoldussen, R. H. Bube, E. A. Fagen, and S. Holmberg, *J. Appl. Phys.* **43**, 1978 (1972).
- ²⁷K. Weiser, R. Fischer, M. H. Brodsky, in *Proceedings of the Tenth International Conference on the Physics of Semiconductors* (U.S. Atomic Energy Commission, Oak Ridge, Tennessee, 1970), p. 667.